Journal of Pharmaceutical Analysis 7 (2017) 411–416

Contents lists available at ScienceDirect

Journal of Pharmaceutical Analysis

journal homepage: www.elsevier.com/locate/jpa

Original Research Article

Simultaneous colorimetric determination of morphine and ibuprofen based on the aggregation of gold nanoparticles using partial least square

Morteza Bahram[a,*], Tayyebeh Madrakian[b], Sakineh Alizadeh[b]

[a] Department of Chemistry, Faculty of Science, Urmia University, 5715175976 Urmia, Iran
[b] Department of Analytical Chemistry, Faculty of Chemistry, Bu-Ali Sina University, 65178638695 Hamadan, Iran

ARTICLE INFO

Keywords:
Morphine
Ibuprofen
Simultaneous determination
AuNPs
Partial least squares

ABSTRACT

In this work a new method is presented for simultaneous colorimetric determination of morphine (MOR) and ibuprofen (IBU) based on the aggregation of citrate-capped gold nanoparticles (AuNPs). Citrate-capped AuNPs were aggregated in the presence of MOR and IBU. The difference in kinetics of AuNPs aggregation in the presence of MOR/IBU was used for simultaneous analysis of MOR and IBU. The formation and size of synthesized AuNPs and the aggregated forms were monitored by infra-red (IR) spectroscopy and transmission electron microscopy (TEM), respectively. By adding MOR or IBU the absorbance was decreased at 520 nm and increased at 620 nm. The difference in kinetic profiles of aggregation was applied for simultaneous analysis of MOR and IBU using partial least square (PLS) regression as an efficient multivariate calibration method. The number of PLS latent variables was optimized by leave-one-out cross-validation method using predicted residual error sum of square. The proposed model exhibited a high capability in simultaneous prediction of MOR and IBU concentrations in real samples. The results showed linear ranges of 1.33–33.29 μg/mL (R^2=0.9904) and 0.28–6.9 μg/mL (R^2=0.9902) for MOR and IBU respectively with low detection limits of 0.15 and 0.03 μg/mL(S/N=5).

1. Introduction

Analytical methods based on spectrophotometric measurements, such as UV–Vis, have attracted increasing interest due to their availability, simplicity and ease of operation [1]. Multivariate spectral calibration is becoming a general method that can be used in quantitative spectral analysis, allowing simultaneous determination of several analytes that coexist in samples with a minimum number of preparation steps [2]. Among multivariate calibration methods, partial least squares (PLS) regression as a powerful method can model the effect of the interfering components without primary separation [2].

Gold nanoparticles (AuNPs) are particularly attractive because they have surface modifying capability such as bio-labelling and are very useful for biological applications. Some unique characteristics of AuNPs are particularly large surface area, good bio-compatibility, high conductivity and electrocatalytic activity [3–5]. AuNPs are also useful colorimetric probes because of their distance-dependent optical properties and extremely high extinction coefficients in visible region that make them more sensitive than AgNPs [6,7]. Due to the localized surface plasmon resonance (LSPR), AuNPs exhibit color shift from red to blue corresponding to their dispersed and aggregated states respectively [8] and based on this, several colorimetric methods have been developed for the detection of biomolecules [9], 2,4,6-trinitrotoluene [10], drugs [9] and melamine [11,12].

Morphine (MOR, Scheme 1A), a non-steroidal anti-inflammatory drug, is used primarily to treat both acute and chronic severe pain. It is also used for pain due to myocardial infarction and for labor pains and its duration of analgesia is about three to seven hours [13].

Ibuprofen (IBU, Scheme 1B), is commonly used as an antipyretic drug especially for podiatry [14]. Many techniques have been applied to the quantitative determination of IBU , including non-aqueous titration [15], polarography [16], colorimetric titration [17], first and second derivative spectrophotometry [18], infra-red (IR) spectrophotometry [19] and H-nuclear magnetic resonance (H-NMR) spectroscopy [20]. In addition, several chromatographic methods have also been employed which although are the most common direct methods, they are time-consuming and in some cases need hazardous organic solvents [21–23].

Various analytical methods have been developed for the determination of MOR. The same as IBU determination, chromatographic methods [24,25] are the most common methods for MOR detection.

Peer review under responsibility of Xi'an Jiaotong University.
* Corresponding author.
E-mail addresses: m.bahram@urmia.ac.ir, morteza.bahram@gmail.com (M. Bahram).

http://dx.doi.org/10.1016/j.jpha.2017.03.001
Received 7 February 2016; Received in revised form 7 March 2017; Accepted 12 March 2017
Available online 14 March 2017

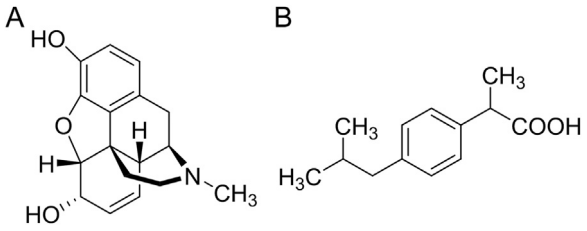

Scheme 1. Structure of (A) morphine and (B) ibuprofen.

Fluorescence [26], enzyme-linked immunosorbent assay [27], immunoassays, such as surface plasmon resonance (SPR) based immunosensors [28] and radioimmunoassays (RIA) [29], molecular imprinting technique [30], amperometric methods [31], chemiluminescence [32] and electrochemical methods [33] are also reported for detection of MOR [34–37].

In this study, a new method is presented for simultaneous determination of MOR and IBU. The method is based on the difference in the aggregation rate of citrate-capped AuNPs in the presence of MOR and IBU. In the presence of MOR or IBU, the absorbance of the solution containing AuNPs decreased at 520 nm and increased at 620 nm, showing the aggregation of AuNPs. Difference in the aggregation kinetics (e.g. absorbance increase versus time at 620 nm) was applied for simultaneous analysis of MOR and IBU using PLS regression as an efficient multivariate calibration method. The proposed method is simple, selective, fast, low cost and in contrast to chromatographic methods, without the need to any sample preparation procedures. This method does not need any expensive apparatus and primary time-consuming separation process by applying the chemometrics methods.

2. Experimental

2.1. Chemicals and materials

All chemicals and reagents used were of analytical grade, solvents were of spectroscopic grade, and double distilled water (DDW) was used throughout the experiments. MOR and IBU pure drugs were obtained from the Department of Food and Drug Administration, Urmia, Iran. All chemicals in the experiments were used without further purification. Sodium citrate, HCl and NaOH were purchased from Merck (Darmstadt, Germany).

2.2. Apparatus

Absorption spectra were recorded with an Agilent 8453 UV–Visible spectrophotometer with 1 cm quartz cells. The size, morphology and structure of the synthesized AuNPs were characterized by transmission electron microscopy (TEM, Philips-CMC-300 kV). A Metrohm pH meter (713 pH-meter) was used for pH measurements. A 40 kHz universal ultrasonic cleaner water bath (Elmasonic E60H, Germany) was used. The calculations were performed in MATLAB (Hyper-cube Inc. Version10) software using PLS files.

2.3. Synthesis of AuNPs

The AuNPS were synthesized according to Ferns method. Briefly, 100 mL of 1 mM aqueous solution of $HAuCl_4$ was heated to boil with stirring; then 10 mL of 1% (m/v) aqueous sodium citrate was added. The color of the mixed solution changed from yellow to wine red in a few minutes, indicating the formation of AuNPs. The boiling and stirring were continued for 15 min [3]. The solution was cooled to room temperature and was stored in a dark bottle at 4 ℃. The solution of the prepared citrate-capped AuNPs was wine red, and had a characteristic localized surface plasmon resonance (LSPR) absorption band of AuNPs at 520 nm (λ_{max}) with narrow peak. In the solution, monodisperse AuNPs were red and exhibited a relatively narrow surface plasmon absorption band centered at around 520 nm in the UV–Vis spectrum. In contrast, a solution containing aggregated AuNPs was blue corresponding to a characteristic red shift in the surface plasmon resonance to higher wavelength of 620 nm [3]. The results are presented in Figs. 1A and B. Figs. 1C and D show the IR spectra of the synthesized AuNPs, before and after aggregation. The concentration of the synthesized nanoparticles was estimated as 10^{-8}mol/L based on the extinction coefficient for 13 nm gold nanoparticles reported in the litratures as 2.8×10^{8}. IR spectra demonstrated the functional groups of PhOH (3000–3600 cm^{-1}), RCOOH (2800–3200 cm^{-1}), OR_2 (1000–1300 cm^{-1}), and Allyl-OH (3000–3600 cm^{-1}). In the spectrum of aggregated AuNPs using the studied drugs, the NR_3 bands (1000–1350 cm^{-1}) obviously exist , proving that drugs interacted with AuNPs. The intensity of IR spectrum of AuNPs decreased when drugs coated them or have interaction with them, while the intensity of the functional group of drug increased. The absorbance spectra of synthesized AuNPs before and after aggregation are shown in Fig. 1E. Fig. 1F represents the time-dependent evolution of UV-Vis spectra of AuNPs toward interaction with MOR.

3. Results and discussion

3.1. Optimization of AuNPs

Ionic strength has a crucial role in the aggregation of nanoparticles. It can be attributed to the ability of strong electrolytes to constrict the aroused electrical double-layer from the capping agent around the nanoparticles. Although the addition of an alectrolyte is necessary for starting the aggregation, it was also found that by increasing the ion strength above a certain limit, the aggregation of nanoparticles occurred even in the absence of analytes [1]. Therefore, the effect of ionic strength (electrolyte concentration) should be studied. The results were presented in Fig. S1 and 1 mmol/L of NaCl was used in the study.

3.2. Optimization of pH

Because of the presence of hydroxyl, carboxyl and amine groups in drugs, pH is another critical parameter that should be taken into consideration. Although electrostatic interactions are dominantly responsible for aggregation of AuNPs [6], the presence of ionizable hydroxyl, carboxyl and amine groups in drugs makes pH another critical parameter which should be considered for optimization and the best results are achieved when the interactions between drugs and AuNPs are strong enough to cause aggregation [38]. Fig. S2 shows the effect of pH on the interaction of drugs with AuNPs. Results showed that the synthesized AuNPs were stable at pH 6 and the drugs had the most favorable ionic structure for interaction with AuNPs in the pH ranges of 6-7. Therefore, pH 6 was chosen for further studies.

3.3. Optimization of incubation time

Different incubation times were examined , and the results showed that AuNPs started to aggregate right after mixing with MOR and IBU in

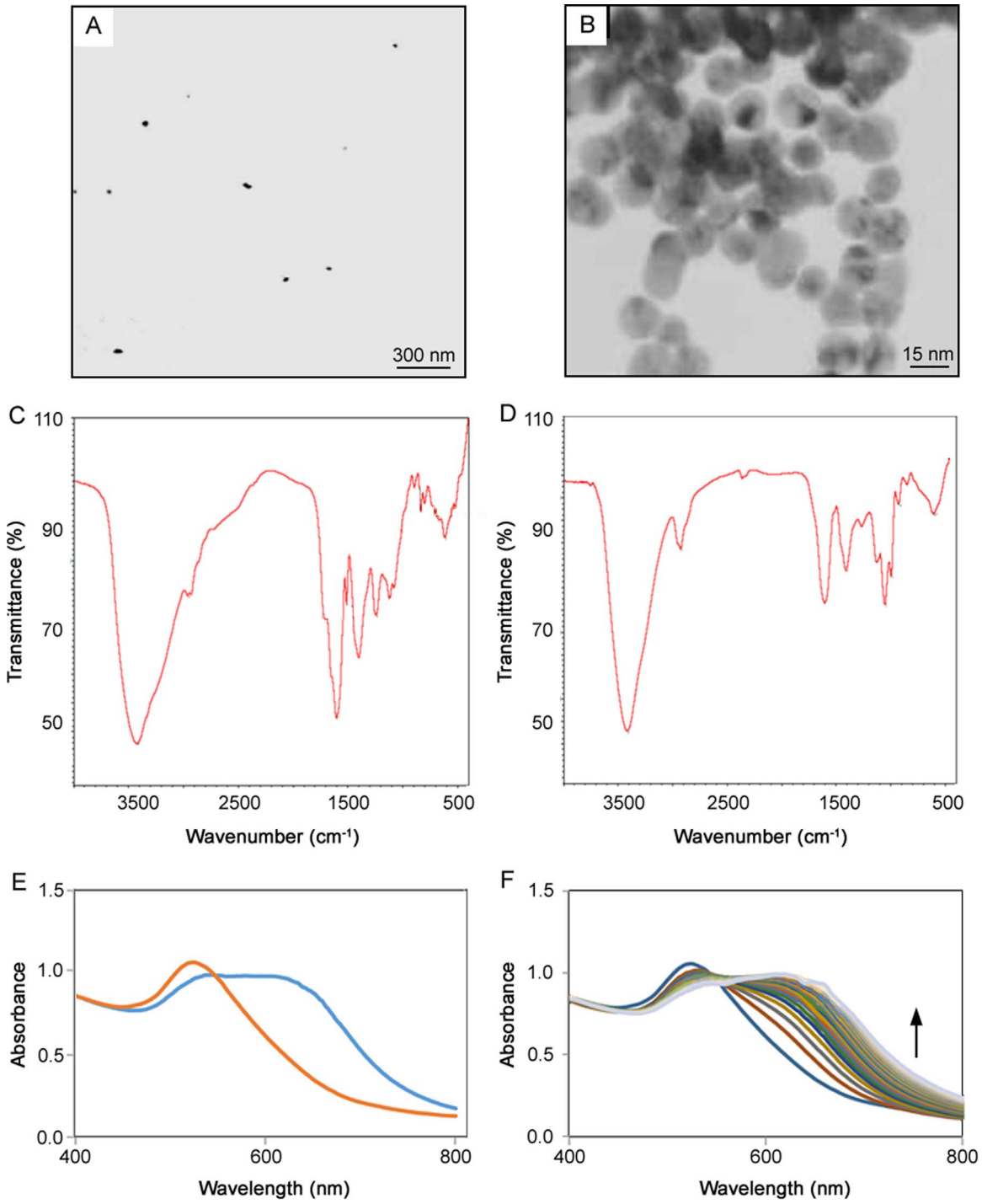

Fig. 1. (A) TEM of synthesized AuNPs, (B) TEM of aggregated AuNPs, (C) IR of aggregated AuNPs, (D) IR of AuNPs, (E) spectrum of synthesized AuNPs and aggregated AuNPs spectrum in optimum condition and (F) aggregation spectra of AuNPs up to 10 min in the presence of 10 μg/mL morphine. Conditions: temperature 25 °C, ionic strength 1 mmol/L and pH 6.

optimum conditions and the aggregation nearly completed after 10 min of incubation which was considered to be the optimum incubation time. So we selected 10 min as the end time for simultaneous kinetic study (Fig. S3).

3.4. The effect of temperature

The results showed that by increasing the temperature the aggregation also increased (Fig. S4). Because the aim of our study was simultaneous kinetic analysis of MOR and IBU using PLS, a temperature should be selected so that a good difference between the kinetic profiles of the analytes is obtained. Based on the results, 25 °C was selected for further experiments.

3.5. PLS model development

PLS calibrations for both drugs were constructed by using nonlinear iterative partial least squares (NIPALS) algorithm. A training set of 27 standard samples (20 samples as calibration set and 7 samples as prediction set) were taken from different mixtures of MOR and IBU.

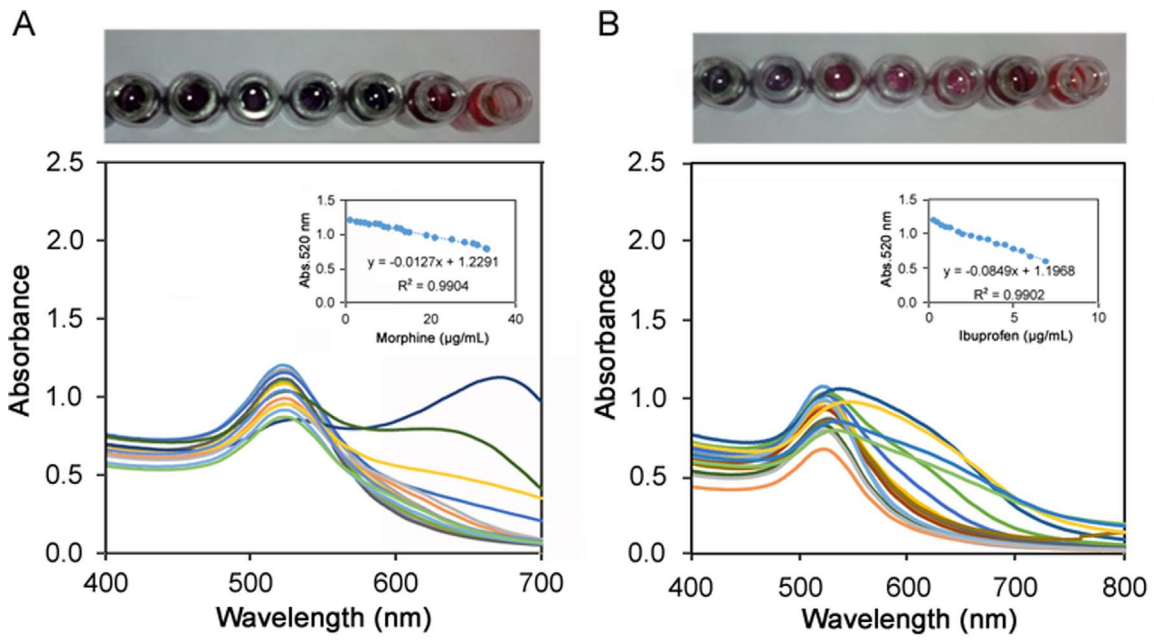

Fig. 2. Calibration curve of (A) morphine of 1.33–33.29 μg/mL and (B) ibuprofen of 0.28–6.9 μg/mL. Conditions: temperature 25 °C, ionic strength 1 mmol/L, reaction time 10 min, pH 6, AuNPs 10 nmol/L.

The correlation between different calibration samples has to be avoided because collinear component in the training set data tends to cause under-fitting in the PLS models [39].

3.6. Linear range of calibration curves

For the mentioned purposes, under optimum experimental conditions, a typical calibration curve was obtained for the determination of MOR and IBU separately. The calibration curves have a linear range of 1.33–33.29 and 0.28–6.9 μg/mL with y=−0.0127x+1.2291, R=0.9904 and y=−0.0849x+1.1965,R=0.9902 (Fig. 2) with the detection limit of 0.15 μg/mL (n=5) and 0.03 μg/mL (n=5) for MOR and IBU, respectively. Table 1 shows a comparison of the results obtained by the present method and those obtained by other methods reported for the determination of these drugs. As can be seen from Table 1, the present method had a good detection limit and linear range compared to those obtained from the reported methods [40–47].

3.7. Simultaneous determination of MOR and IBU

As mentioned above, in order to select the number of factors in PLS algorithm, a cross-validation method leaving out one sample at a time was employed. Increase in the intensity of the absorbance at 620 nm was directly related to the level of MOR and/or IBU in the sample (Fig. 3). Citrate-capped AuNPs were aggregated toward interaction with MOR and IBU with different rate constants. The calibration and prediction sets were collected by monitoring the absorbance increase at 620 nm and were used in PLS process. For the calibration set of 20 sample kinetic profiles, PLS1 and PLS2 algorithms were applied and the amount of the samples left out during the calibration process was calculated. Changes in predicted residual error sum of squares (PRESS) in PLS2 calibration as a function of the number of PLS latent variables are given in Fig. 4. As can be seen from Fig. 4, 3 components were enough to construct the PLS2 model. Nonlinearity in the absorbance–concentration relationship and interaction between the factors could be considered as the other sources of chemical factors.

The predicted values of MOR and IBU levels in the calibration and prediction samples and their corresponding relative prediction errors are listed in Tables 2–4. It was observed that the predicted values were very close to the actual amounts and the relative prediction errors were lower than 5.0%. This confirmed the success of PLS regression for accurate prediction amounts of MOR and IBU in samples. It would be beneficial to evaluate whether the results of PLS1 and PLS2 multivariate calibration resulted in a more appropriate model. For this comparison and the validation of the models, some statistical parameters including root mean square error of prediction (RMSEP), root mean square error of cross validation (RMSECV) and root mean square error of calibration (RMSEC) were calculated and are shown in Table 4. Tables 2 and 3 show that the calibration and prediction results of PLS are more consistent than those of univariate calibration.

The relative standard error and the total relative standard error were calculated using following equations and are shown in Tables 2 and 3.

Table 1
Linear range and limit of detection of the proposed method in comparison with some previous methods for analysis of morphine and ibuprofen.

Compound	Method	Linear range (μg/mL)	LOD (μg/mL)	Reference
Morphine	RP–HPLC	0.15–2	0.05	[41]
	LC–MS–MS	0.002–2	0.001	[42]
	Direct aqueous derivatization	0.008–5.0	0.002	[43]
	GC-MS	0.02–20	0.003	[44]
	Spectrophotometry	0.025–2	0.002	[45]
Ibuprofen	Derivatives of the ratio spectra method	2–32	0.53	[46]
	HPLC	6.1–200	1.7	[47]
	Spectrophotometry	0.28–6.90 (IBU)	0.03 (IBU)	This work
		1.33–33.29 (MOR)	0.15 (MOR)	

RP–HPLC: Reverse phase–high performance liquid chromatography; LC–MS–MS: Liquid chromatography–tandem mass spectrometry; GC–MS: Gas chromatography–mass spectrometry; HPLC: High performance liquid chromatography

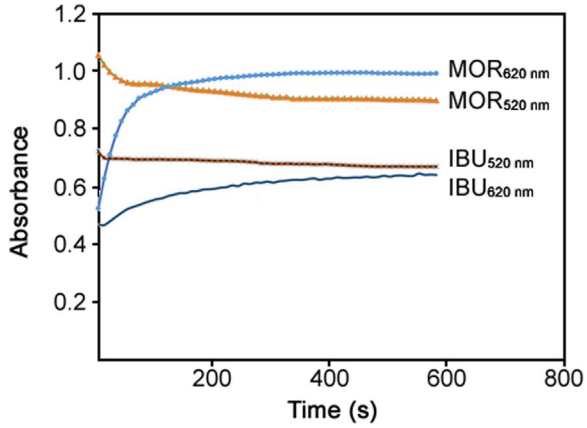

Fig. 3. Change in absorbance of AuNPs at 520 and 620 nm versus time (kinetic profiles) by injection of morphine and ibuprofen. Conditions: morphine/ibuprofen concentration 5.0 μg/mL, temperature 25 °C, ionic strength 1 mmol/L, pH 6, AuNPs 10 nmol/L.

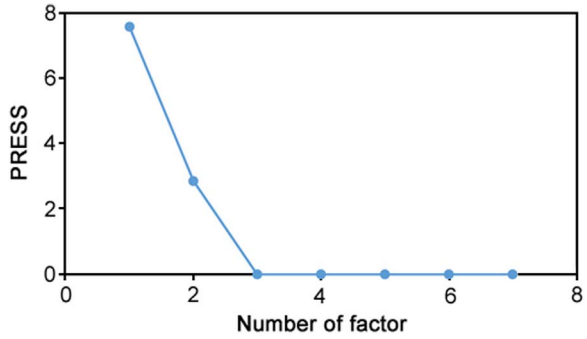

Fig. 4. Plot of PRESS against the number of factors for simultaneous determination of morphine and ibuprofen.

Table 2
The level of IBU and MOR in the prediction set by PLS modeling of kinetic profiles.

Reference value (μg/L)			Predicted value (μg/L)			
No.	IBU	MOR	PLS1		PLS2	
			IBU	MOR	IBU	MOR
1	460	230	418.90	221.50	418.98	221.14
2	530	280	555.06	285.50	555.07	285.49
3	300	160	289.43	156.90	289.46	156.80
4	660	360	652.40	3590	652.40	359.01
5	660	370	663.26	367.70	663.25	367.83
6	580	330	594.99	332.40	594.96	332.57
7	600	330	600.30	333.40	600.35	333.54
R.S.E. (%)			3.55	1.45	3.56	1.49
R.S.E.t (%)						3.19

$$R.\ S.\ E.\ (\%) = \left[\frac{\sum_{J=1}^{N}(C\wedge j - Cj)2}{\sum_{J=1}^{N}(Cj)2}\right]1/2 \times 100$$

$$R.\ S.\ E.\ t(\%) = \left[\frac{\sum_{J=1}^{M}\sum_{J=1}^{N}(C\wedge ij - Cij)2}{\sum_{J=1}^{M}\sum_{J=1}^{N}(Cij)2}\right]1/2 \times 100$$

3.8. Interference effect

The influences of foreign coexisting substances such as naproxen, ascorbic acid, tramadol, codeine, acetaminophen, saccharides, amino acids and ions were tested. As listed in Table S1, some coexisting substances had remarkable interference on the assay. From the results, the interferences of naproxen, ascorbic acid, Na_2NO_2, tryptophan, tyrosine, glucose, sucrose, fructose and lactose were very weak. Among the tested substances K^+, Na^+, NO_3^-, I^-, Cl^-, Mg^{2+}, Fe^{3+}, Ca^{2+}, codeine and cysteine could be present with relatively higher concentrations, but cefexime, ceftriaxone, NH_2OH, Mn^{2+}, Cd^{2+}, SO_4^{2-}, Ca^{2+},Zr^{2+},Co^{2+}, Zn^{2+}, Ni^{2+}, Al^{3+}, Fe^{2+} and Cu^{2+} could only be allowed with relatively low concentrations. The allowed concentrations of these interfering substances, however, were still rather higher than those of MOR and IBU, which indicated that this method had a good selectivity between drugs and other substances.

Table 3
The level of IBU and MOR in the calibration set by PLS modeling of kinetic profiles.

Reference value (μg/L)			Predicted value (μg/L)			
No	IBU	MOR	PLS1		PLS2	
			IBU	MOR	IBU	MOR
1	700	400	704.59	365.16	704.62	365.00
2	520	260	524.96	262.55	524.96	262.54
3	370	190	364.83	190.68	364.83	190.70
4	290	160	293.77	165.03	293.77	165.06
5	320	170	320.16	171.75	320.15	171.77
6	320	170	315.20	173.44	315.20	173.47
7	350	200	346.60	193.80	346.00	193.82
8	460	230	464.14	232.29	464.14	232.28
9	450	270	453.87	274.37	453.87	274.38
10	740	290	737.16	299.62	737.16	299.52
11	180	80	152.70	79.40	152.64	79.94
12	170	100	152.46	103.04	152.49	102.89
13	170	100	172.58	100.65	172.57	100.67
14	330	220	331.50	218.00	331.52	217.95
15	350	200	346.44	199.97	346.44	200.00
16	160	90	162.17	91.43	162.17	91.45
17	240	130	241.60	133.55	241.60	133.56
18	650	370	655.49	376.18	655.49	376.22
19	640	360	639.75	367.63	639.74	367.69
20	200	100	194.34	110.29	194.34	110.34
R.S.E. (%)			1.91	4.03	1.92	4.04
R.S.E. t (%)						2.55

Table 4
Statistical parameters of the PLS1 and PLS2 calibration models developed for simultaneous determination of IBU and MOR with kinetic data.

Statistical parameters	Model of prediction	
	PLS1 (%)	PLS2 (%)
RMSEP	4.7	4.69
RMSECV	4.1	4.2
RMSEC	5.1	5.2

3.9. Real sample analysis

In order to test the applicability of the proposed method, it was applied to determine IBU and MOR in spiked blood serum and urine samples. The constructed PLS model was applied to estimate the concentration of IBU and MOR in these spiked samples. The obtained results showed good recoveries (99.4%–110.7%) (Table S2), and demonstrated the potential applicability of this method for simultaneous determination of IBU and MOR in real samples.

4. Conclusion

The LSPR of the AuNP synthesized by the reduction of gold ion with citrate was, used as a novel analytical tool for the determination of drugs and substances based on the aggregation of AuNPs. A direct relationship was found between the aggregation rates recorded in λ_{max} at about 520 and 620 nm and concentrations of MOR and IBU. Multivariate calibration modeling of the kinetic absorbance data by PLS regression produced accurate results and the relative prediction errors were almost lower than 5%. In comparison with available analytical methods for simultaneous determination of IBU and MOR, the proposed method had following advantages: (i) it needs smaller amounts of reagents; (ii) it is simple, fast, and low-cost; and (iii) in contrast to chromatographic methods, it does not need any expensive apparatus.

Conflicts of interest

The authors declare that there are no conflicts of interest.

Appendix A. Supplementary material

Supplementary data associated with this article can be found in the online version at doi:10.1016/j.jpha.2017.03.001.

References

[1] L. Gao, S. Ren, Prediction of nitrophenol-type compounds using chemometrics and spectrophotometry, Anal. Biochem. 405 (2010) 184–186.
[2] B. Hemmateenejad, A. Abbaspour, H. Maghami, et al., Partial least squares-based multivariate spectral calibration method for simultaneous determination of beta-carboline derivatives in Peganum harmala seed extracts, Anal. Chim. Acta. 575 (2006) 290–299.
[3] K. Hoflich, R.B. Yang, A. Berger, et al., The direct writing of plasmonic gold nanostructures by electron-beam-induced deposition, Adv, Mater 23 (2011) 2657–2661.
[4] Ch. Zeng, Y. Chen, K. Kirschbaum, et al., Structural patterns at all scales in a nonmetallic chiral Au_{133} (SR) $_{52}$ nanoparticle, Sci. Adv. 1 (2015) e1500045.
[5] W. Lu, L. Wang, J. Li, et al., Quantitative investigation of the poly-adenine DNA dissociation from the surface of gold nanoparticles, Sci. Rep. 5 (2015) 158–160.
[6] B. Liu, H. Tan, Y. Chen, Visual detection of silver (I) ions by a chromogenic reaction catalyzed by gold nanoparticles, Microchim. Acta 180 (2013) 331–339.
[7] W. Chansuvarn, A. Imyim, Visual and colorimetric detection of mercury (II) ion using gold nanoparticles stabilized with a dithia-diaza ligand, Microchim. Acta 176 (2012) 57–64.
[8] D. Vilela, M.C. González, A. Escarpa, Sensing colorimetric approaches based on gold and silver nanoparticles aggregation: chemical creativity behind the assay. A review, Anal. Chim. Acta 751 (2012) 24–43.
[9] Y. Xue, H. Zhao, Z. Wu, et al., Colorimetric detection of Cd^{2+} using gold nanoparticles functionalized with 6-mercaptonicotinic acid and L-Cysteine, Analyst 136 (2011) 3725–3730.
[10] Y. Jiang, H. Zhao, N. Zhu, et al., A simple assay for direct colorimetric visualization of trinitrotoluene at picomolar levels using gold nanoparticles, Angew. Chem. Int. Ed. Engl. 47 (2008) 8601–8604.
[11] B. Kong, A. Zhu, Y. Luo, et al., sensitive and selective colorimetric visualization of cerebral dopamine based on double molecular recognition, Angew. Chem. Int. Ed. Engl. 50 (2011) 1837–1840.
[12] K. Ai, Y. Liu, L. Lu, Hydrogen-bonding recognition-induced color change of gold nanoparticles for visual detection of melamine in raw milk and infant formula, J. Am. Chem. Soc. 131 (2009) 9496–9497.
[13] M. S. Hynninen, D.C. H. Cheng, I. Hossain, et al., Non-steroidal anti-inflammatory drugs in treatment of postoperative pain after cardiac surgery, Canad. J Anesthesia, 47 (2000) 1182–1187.
[14] J. Tucci, E. Bandiera, R. Darwiche, et al., Paracetamol and ibuprofen for paediatric pain and fever, J. Pharma. Pract. Res. 39 (2009) 223–225.
[15] V. Larcher, F. Craig, K. Bhogal, et al., Making decisions to limit treatment in life-limiting and life-threatening conditions in children: a framework for practice, Arch. Dis. Child. 100 (2015) s3–23.
[16] A. El-Didamony, S. Hafeez, Spectrophotometric determination of thioridazine hydrochloride in tablets and biological fluids by ion-pair and oxidation reactions, Spectrosc. Int. J. 27 (2012) 129–141.
[17] G. Swaroopa, N. Rani, Polarographic determination of ibuprofen by calibration method using acetic acid and different maxima suppressors, Int. Res. J. of Sci. Eng. 3 (2015) 214–223.
[18] S.M. Diani Saraan, S.M. Sinaga, Muchlisyam, Development method for determination of ternary mixture of paracetamol, ibuprofen and caffeine in tablet dosage form using zero-crossing derivative spectrophotometric, Int. J. Pharm. Tech. Res. 7 (2015) 349–353.
[19] W.S. Hassan, determination of ibuprofen and paracetamol in binary mixture using chemo metric-assisted spectrophotometric methods, Am. J. Appl. Sci. 5 (2008) 1005–1012.
[20] A. El-Brashy, M. Eid, W. Talaat, Kinetic spectrophotometric method for the determination of ibuprofen in pharmaceuticals and biological fluids, Int. J. Biomed. Sci. 2 (2006) 406–413.
[21] M.Q. Al-Abachi, S.A. Al-Safi, Hi.S. Al-Ward, Spectrophotometric kinetic methods for the determination of ibuprofen in pure form and pharmaceutical preparations, Iraq. J. Sci. 56 (2015) 2704–2717.
[22] P.V. Tsouh Fokou, A.K. Nyarko, R. Appiah-Opong, et al., Update on medicinal plants with potency on mycobacterium ulcerans, Bio-Med. Res. Int. 2 (2015) 1–16.
[23] T. Qureshi, N. Memon, S.Q. Memon, et al., Determination of ibuprofen drug in aqueous environmental samples by gas chromatography–mass spectrometry without derivatization, Colum. Int. Pub. Am. J. Mod. Chroma. 1 (2014) 45–54.
[24] S.N. Alvi, A. Yusuf, E. Al Gaai, et al., Rapid determination of ibuprofen concentration in human plasma by high performance liquid chromatography, Word, J. Pharm. Pharmacist. Sci. 3 (2014) 1767–1777.
[25] B.S. Virupaxappa, K.H. Shivaprasad, R.M. Kulkarni, et al., Kinetic estimation of ibuprofen and nimesulide in pharmaceuticals, Asi. J. Res. Chem. 4 (2011) 659–665.
[26] D. Szkutnik-Fiedler, E. Grześkowiak, M. Gaca, et al., HPLC-UV determination of morphine in human plasma and its application to the clinical study, Act. Pol. Pharm. 68 (2011) 473–479.
[27] M. Mabuchi, S. Takatsuka, M. Matsuoka, et al., Determination of morphine, morphine-3-glucuronide and morphine-6-glucuronide in monkey and dog plasma by HPLC-electrospray ionization mass spectrometry, J. Pharm. Biomed. Anal. 35 (2004) 563–574.
[28] J.F. Li, C. Dong, Study on the interaction of morphine chloride with deoxyribonucleic acid by fluorescence method, Spectrochim. Acta A 71 (2009) 1938–1943.
[29] N.F. Atta, A. Gala, S.M. Azab, Electrochemical morphine sensing using gold nanoparticles modified carbon paste electrode, Int. J. Electrochem. Sci. 6 (2011) 5066–5081.
[30] H.X. Hao, H. Zhou, J. Chang, et al., Molecularly imprinted polymers for highly sensitive detection of morphine using surface plasmon resonance spectroscopy, Chin. Chem. Lett. 22 (2011) 477–480.
[31] Y. Gu, X. Yan, C. Li, et al., Biomimetic sensor based on molecularly imprinted polymer with nitroreductase-like activity for morphine detection, Biosens. Bioelectron. 15 (2016) 393–399.
[32] K.C. Ho, C.Y. Chen, H.C. Hsu, et al., Amperometric detection of morphine at a Prussian blue-modified indium tin oxide electrode, Biosens. Bioelectron. 20 (2004) 3–8.
[33] W.M. Yeh, K.C. Ho, Amperometric morphine sensing using a molecularly imprinted polymer-modified electrode, Anal. Chim. Acta 542 (2005) 76–82.
[34] A.M. Idris, A.O. Alnajjar, Exploiting sequential injection analysis technique to automate on-line sample treatment and quantitative determination of morphine in human urine, Talanta 77 (2008) 522–525.
[35] N.F. Atta, A. Gala, A.A. Wassel, et al., Sensitive electrochemical determination of morphine using gold nanoparticles–ferrocene modified carbon paste electrode, Int. J. Electrochem. Sci. 7 (2012) 10501–10518.
[36] A.G. Verstraete, Detection times of drugs of abuse in blood, urine, and oral fluid, Ther. Drug Monit. 26 (2004) 200–205.
[37] M. Sergi, E. Bafile, D. Compagnone, et al., Multiclass analysis of illicit drugs in plasma and oral fluids by LC-MS/MS, Anal. Bioanal. Chem. 393 (2009) 709–718.
[38] K. Wiese Simonsen, A. Steentoft, I.M. Bernhoft, et al., Psychoactive substances in seriously injured drivers in Denmark, Forensic Sci. Int. 224 (2013) 44–50.
[39] J. Conde, J.T. Dias, V. Grazú, et al., Revisiting 30 years of biofunctionalization and surface chemistry of inorganic nanoparticles for nanomedicine, Front. Chem. 2 (2014), http://dx.doi.org/10.3389/fchem.2014.00048.
[40] C. Buzea, I. Ivan, P. Blandino, P.M. Mertes, Nanomaterials and nanoparticles: sources and toxicity, Biointerphases. 2 (2007) MR17–MR71.
[41] A.B. Ruzilawati, W.N. Wan Yusuf, N. Ramli, et al., Determination of morphine in human urine by a simple reverse phase high-performance liquid chromatography method with UV detection, Int. J. Pharm. Sci. Drug Res. 5 (2013) 18–22.
[42] M. Tang, C.K. Ching, M.L. Tse, et al., Surveillance of emerging drugs of abuse in Hong Kong: validation of an analytical tool, Hong Kong Med. J. 21 (2015) 114–123.
[43] B. Rezaei, S. Foroughi-Dehnavi, A.A. Ensafi, Fabrication of electrochemical sensor based on molecularly imprinted polymer and nanoparticles for determination trace amounts of morphine, Ionics 21 (2015) 2969–2980.
[44] S. Chericoni, F. Stefanelli, V. Iannella, et al., Simultaneous determination of morphine, codeine and 6-acetyl morphine in human urine and blood samples using direct aqueous derivatisation: validation and application to real cases, J. Chromatogr. B 949 (2014) 127–132.
[45] X. Zhang, M. Chen, G. Cao, et al., Determination of morphine and codeine in human urine by gas chromatography-mass spectrometry, J. Anal. Methods Chem. , (2013), http://dx.doi.org/10.1155/2013/151934.
[46] C. Stein, K. Comisel, E. Haimerl, et al., Analgesic effect of intraarticular morphine, after arthroscopic knee surgery, N. Engl. J. Med. 325 (1991) 1123–1126.
[47] A.B. Ruzilawati, H. Miran, Validated high performance liquid chromatography method for analysis of methamphetamine in human urine using liquid- liquid extraction, Asian, J. Pharm. Clin. Res. 8 (2015) 199–201.